Mice

Female BALB/c (H-$2^{d,}$ CD45.2) and C57BL/6 (H-2^{b}, CD45.2) mice (BL6), 10-15 weeks of age were purchased from Janvier Laboratories (France). C57BL/6 *Irf4*$^{-/-}$ mice[5] were crossed with C57BL/6-CD5.1-Luc+ (H-2^{b}) mice, which were kindly provided by Andreas Beilhack (Julius-Maximilians-University Würzburg, Germany).

Mouse colonoscopy

For macroscopic assessment of colon integrity colonoscopy was performed with the Mini-Endoscope (Karl Storz). Colitis severity was assessed at day 14 according to a modified murine endoscopic score (MEICS) (1)

Histology

Colon, lung and liver were collected from the mice at day +15/31 after TBI, fixed in 3% paraformaldehyde and embedded in paraffin. Serial histological sections were stained with Hematoxylin/Eosin. Histologic evaluation was performed blinded. Colon evaluation included quantification of apoptotic crypt epithelia cells, granulocytes and the crypt destruction using optical fields of 0.25 mm² (2). The livers were evaluated for portal and periportal inflammation, bile duct damage, hematopoietic islands, prominent granulocytic infiltrates, and inflammatory infiltrate around the central veins. In the lungs the evaluation included peribronchial- and perivascular inflammatory infiltrate, endothelialitis and prominent alveolar macrophages.

Cytokine Analysis

Serum cytokines were analyzed using BD CBA Enhanced Sensitivity Flex Sets (BD Biosciences-Pharmingen). Briefly, standards (0.274 − 200 pg/mL) and samples were incubated with capture bead mixture, mouse detection reagent and enhanced sensitivity detection reagent in 96-well plates at room temperature in the dark for 1h. After washing, samples were measured with a BD FACS Verse™ cytometer (BD Bioscience-Pharmingen, USA). FCAP Array Software (BD Bioscience-Pharmingen, USA) was used to analyze the data.

RNA sequencing analysis

Transcripts with less than 5 read counts per sample were filtered and p-values were corrected for multiple testing using the Benjamini-Hochberg (BH) procedure. A gene was considered differentially expressed if BH < 0.05. The functional enrichment analysis (GO term) was performed with ClusterProfiler R package. STRING analysis was performed with STRING database v.11 and Cytoscape v.3.2.1.

Mixed lymphocyte reaction and Immunoblot

MACS (Miltenyi) isolated $CD4^{+}$ T cells from *Irf4*$^{-/-}$ or WT mice splenocytes were co-incubated with allogenic BALB/c BM-derived dendritic cells (DCs) in a DC/T cell ratio of 1:2. For protein isolation, cells were harvested before and at day 10 of co-culture. At day 10 living $CD4^{+}$ T cells were enriched via flow-cytometry based sorting, using anti-CD4 BV-605 (Biolegend) antibody and 7-AAD. Cells were lysed in RIPA-buffer and yielded protein was separated in a 12% SDS-Gel and blotted on a PVDF membrane. Immunodetection of IRF4 and BACH2 was performed with the following primary and horseradish peroxidase (HRP)- linked secondary IgG antibodies: rat-anti-IRF4 (clone 3E4, Santa Cruz, sc-130921, 1:200); rat-anti-BACH2 (clone 7A4, Abcam, 1:10000); rabbit-anti-ß-Actin (clone D6A8, Cell Signaling, 1:5000); goat-anti-rat HRP (polyclonal, 31470, Invitrogen, 1:10000) or goat-anti-rabbit IgG-HRP (Cell Signaling, #7074, 1:10000).

Biopsy characteristics

Biopsies were obtained either during screening study in asymptomatic patients or because of clinical symptoms indicative of de novo onset or persistence/recurrence of acute intestinal GVHD. Biopsies were obtained by upper GI or lower GI endoscopy or sigmoidoscopy. Overall, 4 biopsies were obtained from duodenum, 11 from Ileum or upper caecum, 19 from colon and 75 from sigmoid colon. For analysis, biopsies from different intestinal compartments were used since homogenous expression of IRF4 and BACH2 was proven throughout the different locations (Supplementary Figure 4A).

Donor lymphocyte isolation and activation

For *in vitro* studies $CD4^+$ T cells were isolated from buffy coats by Rosette Sep negative $CD4^+$ T cell isolation kit (Stemcell). Plates were pre-coated with anti-human CD3 (OKT-3, InVivoMab, 10µg/mL) and $CD4^+$ T cells were cultivated with 2 mg/mL anti-human CD28 (CD28.2, Biolegend), 100 IU/ml human IL-2 (Novartis) and either 0.25 mM Methylprednisolone (URBASON® solubile forte, Sanofi), 2.4 µM Cyclosporine A (Sandimmun®, Novartis), a combination of both, or none of them for three days. For unstimulated controls, no anti-CD28 was added. RNA was extracted by peqGold Total RNA Kit (Peqlab).

Immunohistochemistry

2-3µm thick slides sectioned from the formalin-fixed and paraffin-embedded (FFPE) biopsies were stained, treated with CC1 buffer, and detection of FoxP3 was performed with a monoclonal mouse antibody (1:120, eBioscience 14-4777, clone 236A/E7) and OptiView DAB IHC Detection Kit (Ventana). The mean number of FoxP3-positive stromal cells was determined microscopically per high power field (HPF) with a Zeiss Axioskop 40 microscope (Zeiss), counting 3-12 HPF exhibiting the highest histological GVHD damage.

Study approval

All mouse experiments were approved by the government committee (Regierungspräsidium Darmstadt, Germany) and conducted in accordance with the requirements of the German Animal Welfare Act. The patient biopsy studies and scientific analysis were approved by the local ethical review board (approval no 02/220 and 09/059) and were performed in accordance with the regulations of Helsinki. All patients consented for biopsy.

References

1. Becker C, Fantini MC, Neurath MF. High resolution colonoscopy in live mice. *Nature protocols*. 2006;1(6):2900-2904. doi:10.1038/nprot.2006.446.
2. Kaplan DH, Anderson BE, McNiff JM, Jain D, Shlomchik MJ, Shlomchik WD. Target antigens determine graft-versus-host disease phenotype. *Journal of immunology (Baltimore, Md. : 1950)*. 2004;173(9):5467-5475. doi:10.4049/jimmunol.173.9.5467.

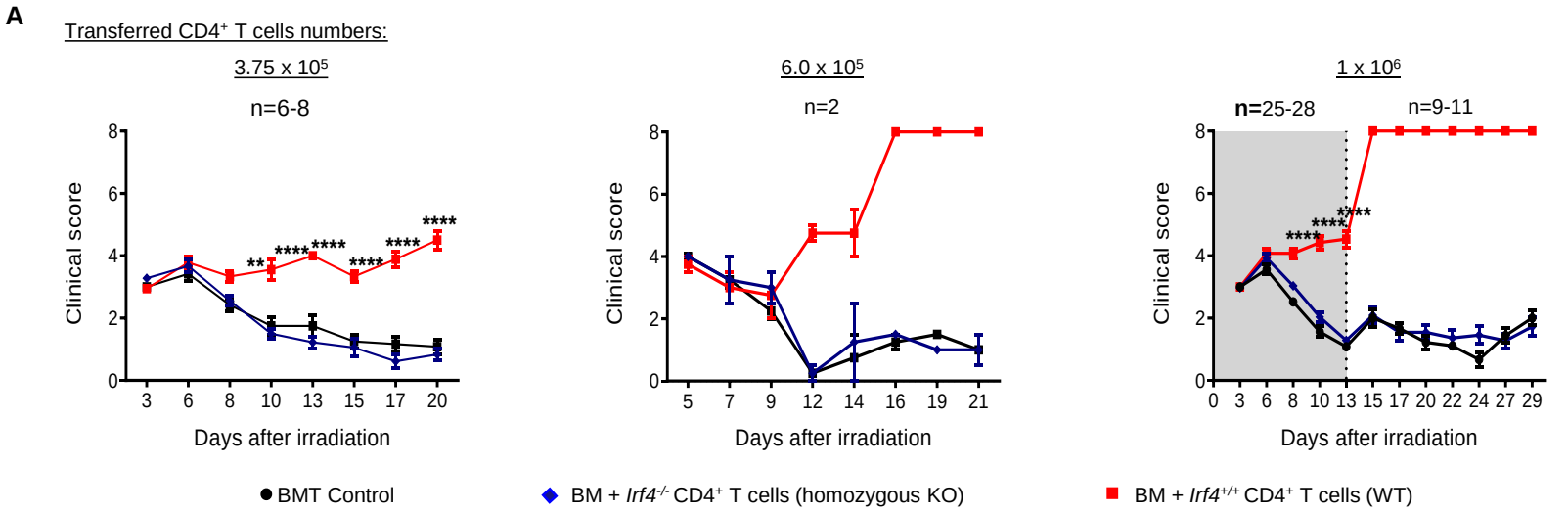

Figure S1: *Irf4*$^{-/-}$ CD4^{+} T cell induce less aGVHD and aGVHD associated colitis to later time points in a dose independent manner.

Lethally irradiated BALB/c recipients that received 5x10^{6} CD45.2^{+} WT BL/6 BM depleted for CD90.2+ cells at day one and different concentrations of CD4^{+} CD45.1^{+} Luciferase^{+} T cells from WT, *Irf4*$^{-/-}$ or *Irf4*$^{+/-}$ donors with BL/6 background at day two were monitored every 2-3 days for clinical GVHD score (A). The colons of BM and *Irf4*$^{-/-}$ CD4^{+} T cell recipients were analyzed at day 30/31 post irradiation by colonoscopy (B) and by histopathological scoring (C). One representative picture is shown per condition. (D) Inflammatory responses in the recipients at day 15 post irradiation were monitored by CBA-based measurement of pro- and anti-inflammatory cytokines in the serum. Data represent the mean ± standard deviation combined from 1-4 independent experiments (BM =4, *Irf4*$^{-/-}$ =2, *Irf4*$^{+/-}$ =1, WT =4 experiments). Data represent the mean + standard deviation combined from independent experiments. If applicable, all data points each representing an individual are shown. **P < .01, ***P < .005, **** P < .0001.

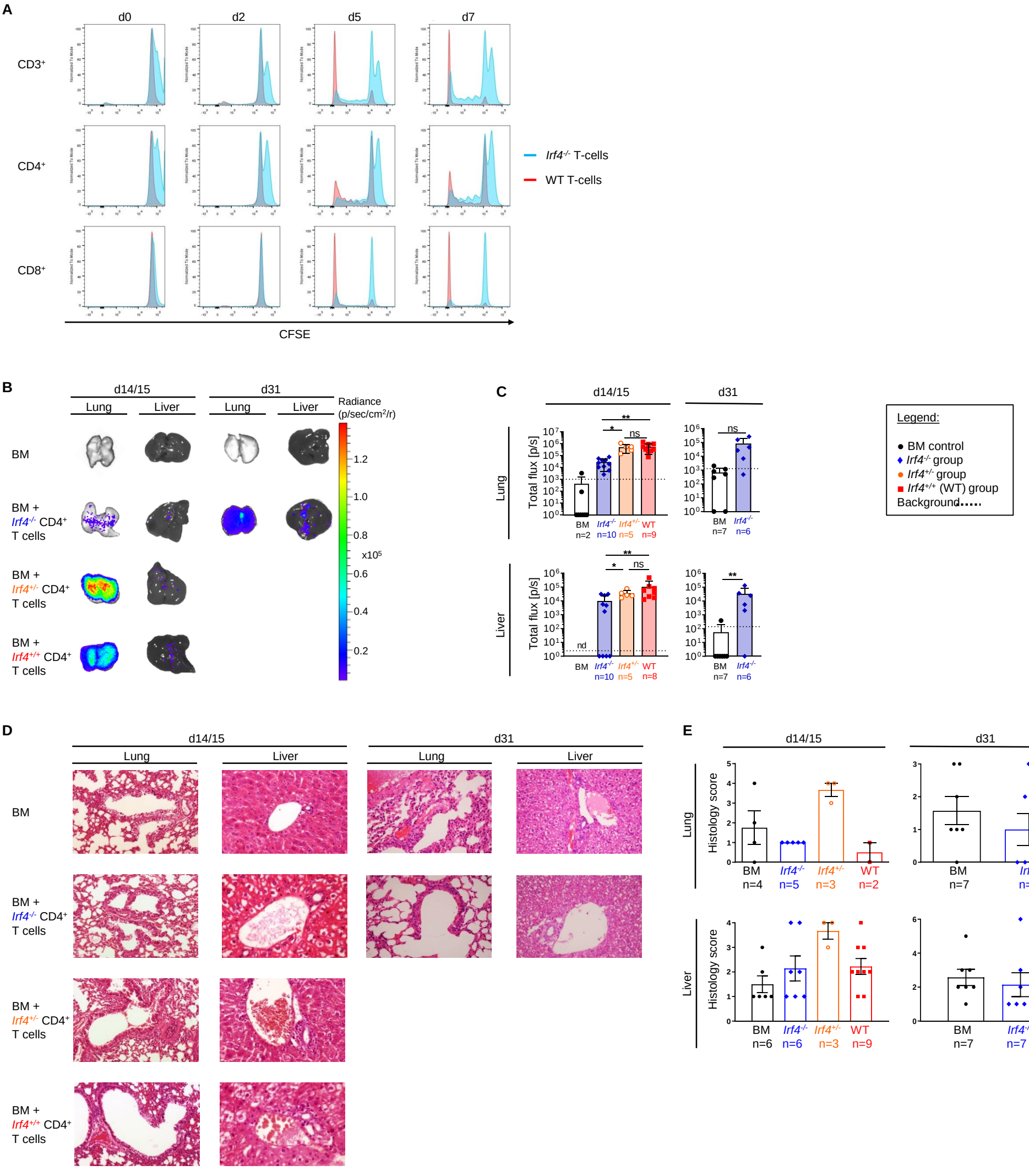

Figure S2: *Irf4*$^{-/-}$ CD4^{+} T cells show decelerated proliferation but migrate to the same aGVHD target organs like WT and *Irf4*$^{+/-}$ CD4^{+} T cells.

(A) Proliferation of *Irf4*$^{-/-}$ T cells versus WT T cells was monitored via CFSE decrease over time, by stimulation of isolated T cells (BL/6 background derived) with dendritic cells (Balb/c background derived) in a mixed lymphocyte reaction. The migration of 1x10^{6} CD4^{+} CD45.1^{+} Luciferase^{+} T cells from WT, *Irf4*$^{-/-}$ or *Irf4*$^{+/-}$ donors with BL/6 background in the lethally irradiated WT BL/6 CD0.2-depleted BM transplanted recipients was traced by imaging of the Luc^{+} CD4^{+} T cells in the in the GVHD target organs lung and liver after dissection at day 14/15 and day 31 after irradiation. Representative BLI pictures (A) and measured BLI signals (B) for the respective groups are shown. Histological sections of lungs and livers were additionally stained with Haematoxilin/Eosin (HE) and scored for histopathological changes (D-E).

Data represent the mean ± standard deviation combined from independent experiments. If applicable, all data points each representing an individual are shown. **P < .05, **P < .01.* Analyses were performed with the two tailed Mann-Whitney test.

Supplemental Figure 3

A

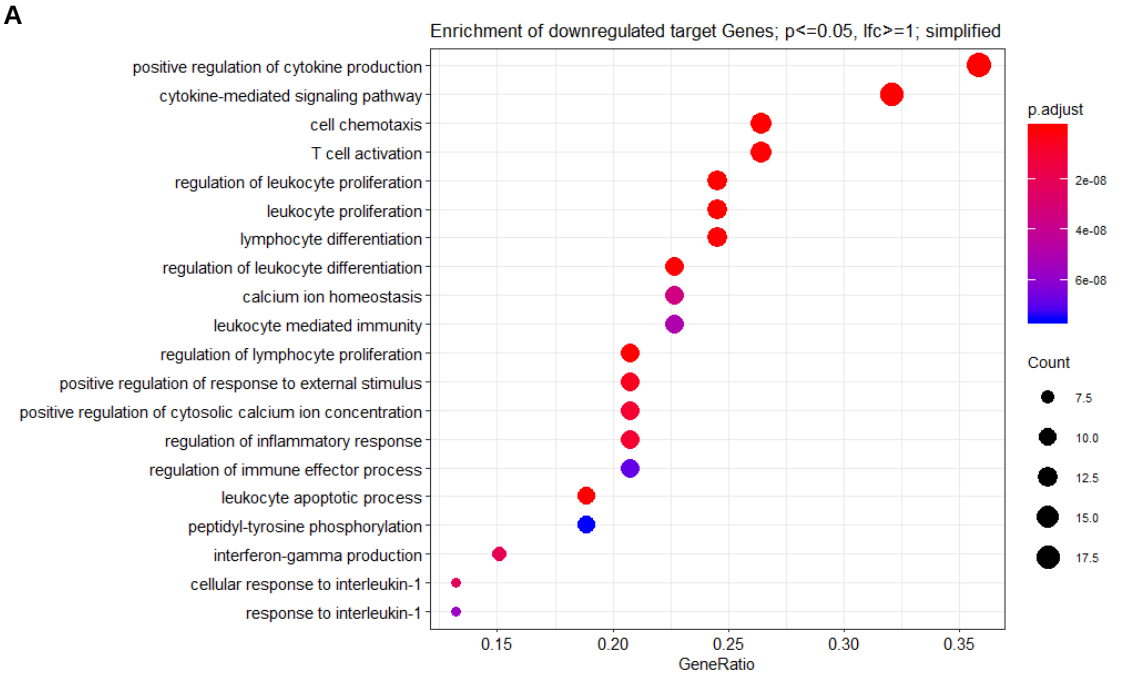

B

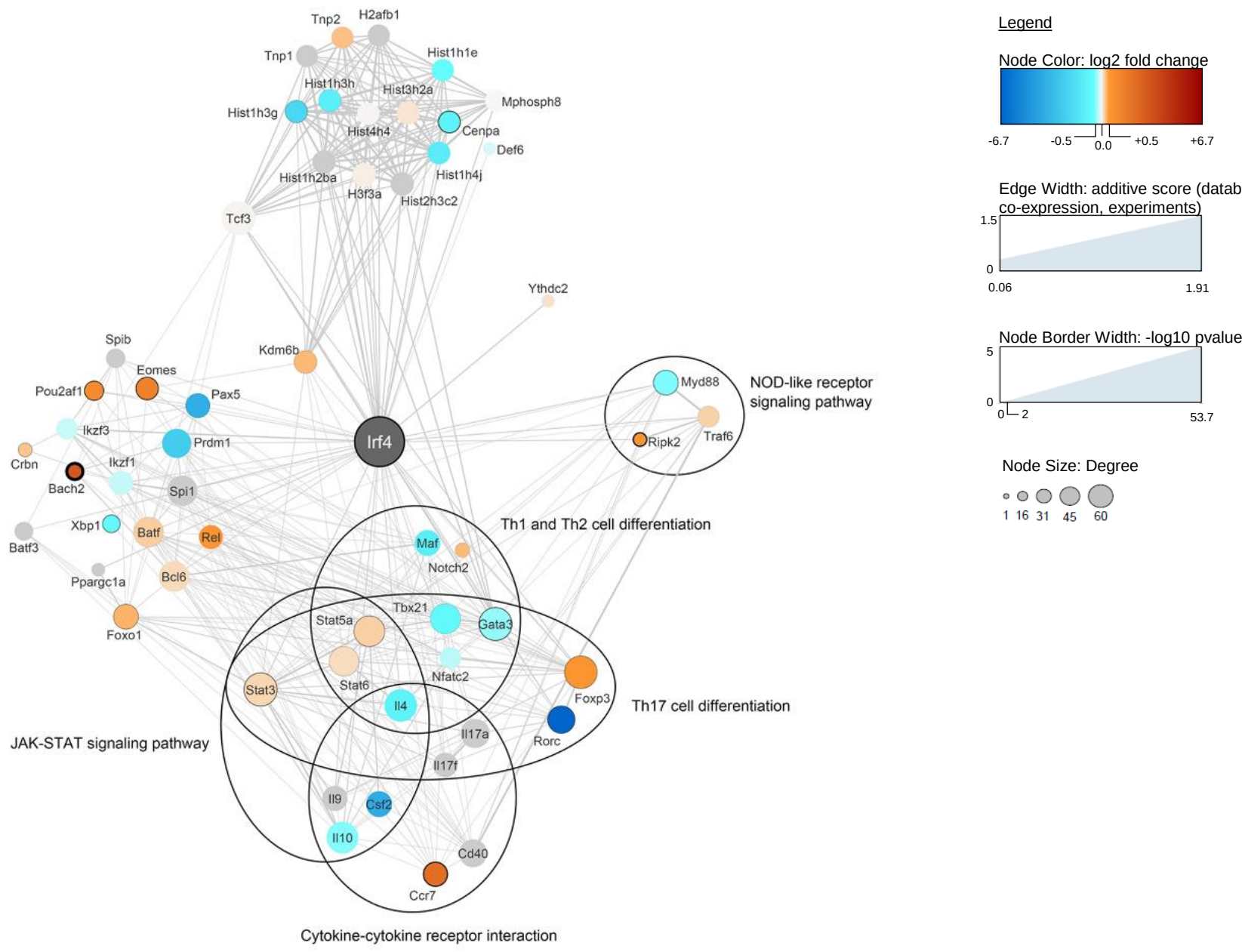

C

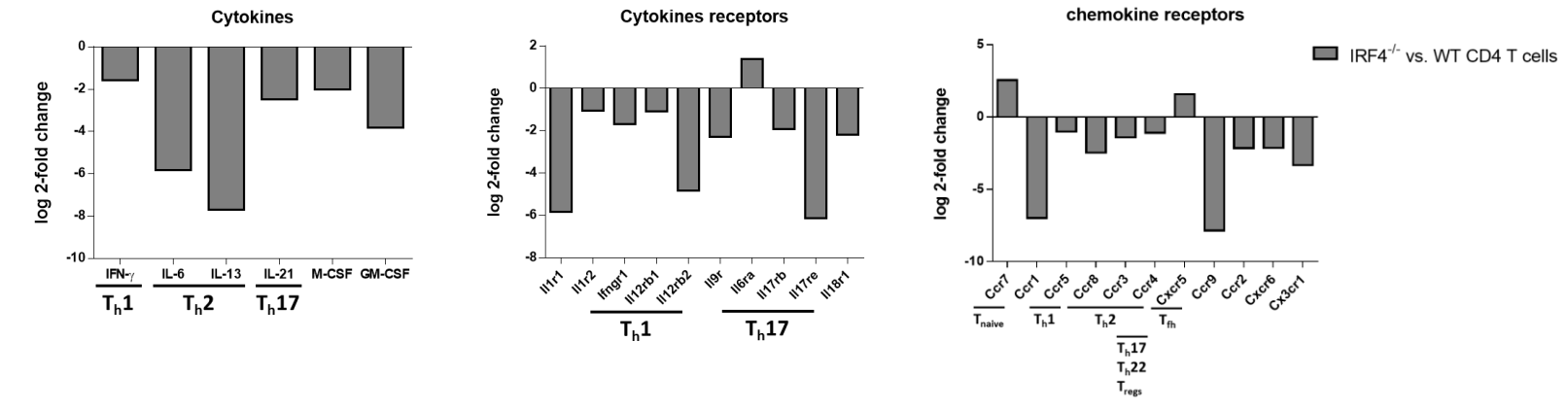

Figure S3: STRING analysis of interacting proteins with murine IRF4 impaired Th differentiation and *Irf4*$^{-/-}$ CD4^{+} T cell according to GO term enrichment analysis and expression of Th specific cytokines, cytokine receptors and chemokine receptors.

Lethally irradiated BALB/c recipients received 5x10^{6} CD45.2^{+} WT C57BL/6 BM depleted for CD90.2^{+} cells at day one and 1x10^{6} CD4^{+} CD45.1^{+} Luciferase^{+} T cells from *Irf4*$^{-/-}$ or *Irf4*$^{+/-}$ donors with C57BL/6 background at day two. CD4^{+} T cells were re-isolated and sorted for CD45.1^{+} CD4^{+} T cells with high purity and RNA was extracted from these cells for RNA sequencing analysis. (A) GO term enrichment analysis of downregulated genes between *Irf4*$^{-/-}$ and *Irf4*$^{+/-}$ recipients was performed with p-value<0.05. (B) The 60 most probable IRF4 protein-protein interactors were identified by STRING database analysis (all active interaction sources included, minimum required interaction score = medium confidence (0.400), max number of interactors=60). Results of differential gene expression analysis from RNA sequencing were plotted onto the STRING network using Cytoscape: Fold-change are depicted by node-colour, p-value by node-border width, node-degree (i.e. cumulative number of interactions) by node size and the interaction score based on the additive score of interaction scores for experiments, databases and co-expression sources as edge width. Predicted interactors with an additive interaction score to IRF4 of 0 which did not have any other interaction partner with an additive score >0 are not displayed in the network. KEGG pathways and the respective proteins involved are labeled by circles.

(C) Expression of genes coding for chemokine receptors, cytokines and cytokine receptors specific for Th-1, Th-2 and Th-17 between *Irf4*$^{+/-}$ and *Irf4*$^{-/-}$ CD4+ T cells was plotted was plotted by the mean of 2-fold change + standard deviation.

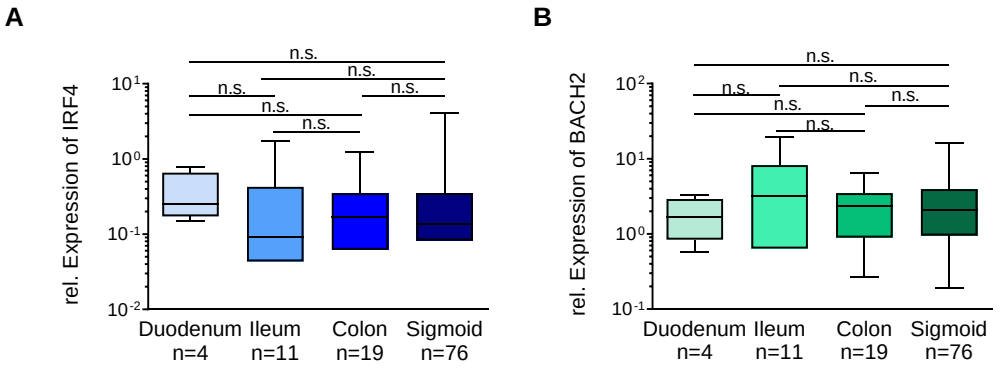

Figure S4: Homogenous expression of *IRF4* and *BACH2* throughout biopsies form different intestinal compartments.

Relative expression of *IRF4* (A) and *BACH2* (B) in biopsies from GVHD patients from different intestinal compartments including duodenum, ileum, colon and sigma quantified by qPCR. Whisker-box plots indicate the mean, min and max value of individual sample sizes indicated in the respective plots. *P < .05, **P < .01, ***P < .001, ****P < .0001. Analyses were performed with the two tailed Mann-Whitney test.

Table S1: Summary of patients' characteristics

Age in years		**mean**	**(range)**
	Patients (N=76)	53	(20-69)
Sex		**n**	**(%)**
	male	45	59.2
	female	31	40.8
Diagnosis			
	Acute leukemia	41	53.9
	Myelodysplastic syndrome	10	13.2
	Myeloproliferative syndrome	3	3.9
	Lymphoma	22	28.9
Stage of underlying disease			
	early	15	19.7
	intermediate	27	35.5
	advanced	34	44.7
Donor type			
	Unrelated donor	49	64.5
	Sibling	24	31.6
	Haploidentical donor	3	3.9
Stem cell source			
	PBSC	71	93.4
	BM	5	6.6
Conditioning regimen			
	Reduced intensity	68	89.5
	Standard	8	10.5
Conditioning regimen in detail			
	FBM	31	40.8
	FTM	6	7.9
	Thio/Treo/Flud	2	2.6
	Treo/Flud	12	15.8
	Thio/Flud	1	1.3
	Mel/Treo/Flud	5	6.6
	TBI/Flud	4	5.3
	TBI/Cy2	2	2.6
	FLAMSA-RIC/Treo	2	2.6
	FLAMSA-RIC	3	3.9
	TBI/Etoposid	1	1.3
	TBI/Mel/Flud	2	2.6
	Busulfan/Flud	1	1.3
	Treo/Cy2/Eto	1	1.3
	FBM+PostTxCy2	2	2.6
	Thiotepa+PostTxCy2	1	1.3
Immunosuppression			
	CyA/MTX	58	76.3
	CyA/MMF	13	17.1
	Everolimus	1	1.3
	Tacro/MMF	1	1.3
	PostTxCy/Tacro/MMF	3	3.9

Table S2: qPCR primer sequences for the respective transcripts

Target Gene	Forward Primer (5'-3')	Reverse Primer (5'-3')
18S	ACCGATTGGATGGTTTAGTGAG	CCTACGGAAACCTTGTTACGAC
IRF4	GACAACGCCTTACCCTTCG	GGGACATTGGTACGGGATTT
BACH2	GCACAGGACCTGGAAAAATTA	TTCCGCTGGTCATTGAGG
NLRP3	GGACTGAAGCACCTGTTGTGC	TCCTGAGTCTCCCAAGGCATTC

Table S3: Predicted KEGG pathways for murine IRF4 STRING protein-protein interaction network

# background	# genes	category	description	FDR value	genes	network.SUID	nodes.SUID	p-value	transferred FDR value
100	12	KEGG Pathways	Th17 cell differentiation	2.23E-14	10090.ENSMUSP00000000889|10090.ENSMUSP00000001484|10090.ENSMUSP00000004145|10090.ENSMUSP00000021784|10090.ENSMUSP00000027061|10090.ENSMUSP00000029795|10090.ENSMUSP00000046960|10090.ENSMUSP00000074198|10090.ENSMUSP00000089708|10090.ENSMUSP00000100	692	750|725|710|759|742|714|705|738|744|743|753|752	2.21E-16	1.365169514
167	12	KEGG Pathways	Transcriptional misregulation in cancer	2.27E-12	10090.ENSMUSP00000002180|10090.ENSMUSP00000014174|10090.ENSMUSP00000017799|10090.ENSMUSP00000019060|10090.ENSMUSP00000023151|10090.ENSMUSP00000055308|10090.ENSMUSP00000099928|10090.ENSMUSP00000100979|10090.ENSMUSP00000104732|10090.ENSMUSP00000124	692	756|739|735|717|754|731|730|758|703|728|722|727	6.75E-14	1.164397414
92	9	KEGG Pathways	Systemic lupus erythematosus	2.17E-10	10090.ENSMUSP00000016673|10090.ENSMUSP00000017799|10090.ENSMUSP00000056604|10090.ENSMUSP00000100618|10090.ENSMUSP00000104445|10090.ENSMUSP00000124509|10090.ENSMUSP00000135215|10090.ENSMUSP00000136357|10090.ENSMUSP00000140394	692	749|735|748|745|719|728|722|732|727	8.58E-12	0.966354027
86	8	KEGG Pathways	Th1 and Th2 cell differentiation	3.90E-09	10090.ENSMUSP00000000889|10090.ENSMUSP00000001484|10090.ENSMUSP00000004145|10090.ENSMUSP00000074198|10090.ENSMUSP00000078741|10090.ENSMUSP00000089708|10090.ENSMUSP00000100041|10090.ENSMUSP00000104732	692	750|725|710|738|707|744|743|703	1.93E-10	0.840893539
161	7	KEGG Pathways	Jak-STAT signaling pathway	5.75E-06	10090.ENSMUSP00000000889|10090.ENSMUSP00000004145|10090.ENSMUSP00000016673|10090.ENSMUSP00000019060|10090.ENSMUSP00000022019|10090.ENSMUSP00000089708|10090.ENSMUSP00000120152	692	750|710|749|717|736|744|752	3.99E-07	0.524033216
252	8	KEGG Pathways	Cytokine-cytokine receptor interaction	7.13E-06	10090.ENSMUSP00000000889|10090.ENSMUSP00000016673|10090.ENSMUSP00000017799|10090.ENSMUSP00000019060|10090.ENSMUSP00000022019|10090.ENSMUSP00000027061|10090.ENSMUSP00000046960|10090.ENSMUSP00000099423	692	750|749|735|717|736|742|705|734	5.65E-07	0.514691047
91	5	KEGG Pathways	IL-17 signaling pathway	6.89E-05	10090.ENSMUSP00000000889|10090.ENSMUSP00000004949|10090.ENSMUSP00000019060|10090.ENSMUSP00000027061|10090.ENSMUSP00000046960	692	750|712|717|742|705	6.82E-06	0.416178078
269	7	KEGG Pathways	HTLV-I infection	9.86E-05	10090.ENSMUSP00000002180|10090.ENSMUSP00000004145|10090.ENSMUSP00000017799|10090.ENSMUSP00000019060|10090.ENSMUSP00000054852|10090.ENSMUSP00000074198|10090.ENSMUSP00000100979	692	756|710|735|717|706|738|758	1.07E-05	0.400612309
107	5	KEGG Pathways	Toxoplasmosis	1.20E-04	10090.ENSMUSP00000004949|10090.ENSMUSP00000016673|10090.ENSMUSP00000017799|10090.ENSMUSP00000035092|10090.ENSMUSP00000120152	692	712|749|735|751|752	1.45E-05	0.392081875
132	5	KEGG Pathways	Measles	3.00E-04	10090.ENSMUSP00000000889|10090.ENSMUSP00000004145|10090.ENSMUSP00000004949|10090.ENSMUSP00000035092|10090.ENSMUSP00000120152	692	750|710|712|751|752	3.82E-05	0.352287875
69	4	KEGG Pathways	Acute myeloid leukemia	3.30E-04	10090.ENSMUSP00000002180|10090.ENSMUSP00000004145|10090.ENSMUSP00000019060|10090.ENSMUSP00000120152	692	756|710|717|752	4.95E-05	0.348148606
143	5	KEGG Pathways	Hepatitis B	3.50E-04	10090.ENSMUSP00000004145|10090.ENSMUSP00000035092|10090.ENSMUSP00000074198|10090.ENSMUSP00000089708|10090.ENSMUSP00000120152	692	710|751|738|744|752	5.53E-05	0.345593196
158	5	KEGG Pathways	Necroptosis	5.20E-04	10090.ENSMUSP00000004145|10090.ENSMUSP00000089708|10090.ENSMUSP00000100618|10090.ENSMUSP00000104445|10090.ENSMUSP00000120152	692	710|744|745|719|752	8.73E-05	0.328399666
522	8	KEGG Pathways	Pathways in cancer	5.60E-04	10090.ENSMUSP00000000889|10090.ENSMUSP00000002180|10090.ENSMUSP00000004145|10090.ENSMUSP00000004949|10090.ENSMUSP00000055308|10090.ENSMUSP00000078741|10090.ENSMUSP00000089708|10090.ENSMUSP00000120152	692	750|756|710|712|731|707|744|752	9.98E-05	0.325181197
100	4	KEGG Pathways	T cell receptor signaling pathway	0.001	10090.ENSMUSP00000000889|10090.ENSMUSP00000016673|10090.ENSMUSP00000019060|10090.ENSMUSP00000074198	692	750|749|717|738	2.00E-04	0.3
199	5	KEGG Pathways	Viral carcinogenesis	0.0012	10090.ENSMUSP00000004145|10090.ENSMUSP00000056604|10090.ENSMUSP00000099928|10090.ENSMUSP00000120152|10090.ENSMUSP00000136357	692	710|748|730|752|732	2.50E-04	0.292081875
40	3	KEGG Pathways	Intestinal immune network for IgA production	0.0012	10090.ENSMUSP00000000889|10090.ENSMUSP00000016673|10090.ENSMUSP00000017799	692	750|749|735	2.30E-04	0.292081875
132	4	KEGG Pathways	FoxO signaling pathway	0.0022	10090.ENSMUSP00000016673|10090.ENSMUSP00000023151|10090.ENSMUSP00000055308|10090.ENSMUSP00000120152	692	749|754|731|752	5.40E-04	0.265757732
100	3	KEGG Pathways	AGE-RAGE signaling pathway in diabetic complications	0.0095	10090.ENSMUSP00000004145|10090.ENSMUSP00000055308|10090.ENSMUSP00000120152	692	710|731|752	0.0029	0.202227639
31	2	KEGG Pathways	African trypanosomiasis	0.0111	10090.ENSMUSP00000016673|10090.ENSMUSP00000035092	692	749|751	0.0037	0.195467702
122	3	KEGG Pathways	Osteoclast differentiation	0.0144	10090.ENSMUSP00000002180|10090.ENSMUSP00000004949|10090.ENSMUSP00000074198	692	756|712|738	0.005	0.184163751
164	3	KEGG Pathways	NOD-like receptor signaling pathway	0.031	10090.ENSMUSP00000004949|10090.ENSMUSP00000035092|10090.ENSMUSP00000038833	692	712|751|726	0.0111	0.150863831
71	2	KEGG Pathways	Adipocytokine signaling pathway	0.0449	10090.ENSMUSP00000117040|10090.ENSMUSP00000120152	692	724|752	0.0174	0.134775366
203	3	KEGG Pathways	Kaposi's sarcoma-associated herpesvirus infection	0.0476	10090.ENSMUSP00000019060|10090.ENSMUSP00000074198|10090.ENSMUSP00000120152	692	717|738|752	0.0193	0.132239305
78	2	KEGG Pathways	Salmonella infection	0.0496	10090.ENSMUSP00000019060|10090.ENSMUSP00000035092	692	717|751	0.0206	0.130451832